

Separation of gas mixtures in unsteady-state conditions

I.N. Beckman**, A.B. Shelekhin

Chair of Chemical Technology, Chemistry Department, Moscow State University, Moscow (USSR)

V.V. Teplyakov

A. V. Topchiev Institute of Petrochemical Synthesis, The USSR Academy of Sciences, Moscow (USSR)

The prospects for the application of unsteady-state boundary conditions at the membrane inlet for increasing the selectivity of gas separation are discussed in this paper. The phenomena occurring upon passage of a concentration pulse and two-gas-component penetrant concentration waves through the membrane have been investigated. It has been shown that pulsed supply of the mixture to be separated at the membrane inlet increases the separation coefficients by a factor of several orders owing to differences in the diffusion coefficients of the gas mixture components in the membrane. Sinusoidal boundary conditions at the membrane inlet allow filtration of the amplitude of the total output oscillations from the signal of the component with a low diffusion coefficient (in this case the membrane acts as a frequency filter), which can be employed for increasing the selectivity of the sensors. The proposed techniques are exemplified by separation of the He/CO₂ gas mixture on a polymeric polyvinyltrimethylsilane (PVTMS) membrane.

Introduction

At present, the membrane separation of gas mixtures is performed exclusively in steady-state conditions. The effectiveness of the gas separation process in this case is determined mainly by the transport characteristics of the membrane material.

The purpose of the present communication is to consider the prospects for application of unsteady-state boundary conditions for experiments (a pulsed version of the permeability method and the method of concentration waves) on membrane separation of gas mixtures. Theoretical aspects of the method are considered. Experimental testing of the method is exemplified by the separation of the He/CO₂ mixture in the process of diffusion across polyvinyltrimethylsilane (PVTMS) films.

Theoretical considerations

Separation of gas mixtures under pulsed conditions

When a pulsed version of the permeability method is employed, the square concentration pulse is sent to the membrane inlet and the pulse distortions occurring in the diffusion process are measured [1,2]. If the square pulse duration is At , the time dependence of the gas flux at the membrane outlet is expressed by the equation:

$$J(t) = J_{\infty} [f(u) - f(u - D\Delta t/l^2)] \quad (1)$$

$$J_{\infty} = DC_0 S/l$$

where $u = \frac{Dt}{l^2}$ and $C_0 = P_0 \sigma$

$\alpha = 0$ for $u < \frac{D\Delta t}{l^2}$ - is the ascending part of the curve

and

$\alpha = 1$ for $u > \frac{D\Delta t}{l^2}$ - is the descending part of the curve

$$f(u) = 1 + 2 \sum_{n=1}^{\infty} (-1)^n \exp(-n^2 \pi^2 u) = \frac{2}{\sqrt{u\pi}} \sum_{n=1}^{\infty} \exp\left(-\frac{n-0.5}{u}\right) \quad (2)$$

The dependence of the exiting pulse amplitude on its time duration is given in Fig. 1. It is seen that the membrane productivity decreases with decreasing time duration.

In the case of short pulse ($\Delta t \rightarrow 0$), we have:

$$J(t) = 2J_\infty \Delta t \sum_{n=1}^{\infty} (-1)^n n^2 \pi^2 u \exp(-n^2 \pi^2 u) \quad (3)$$

The time of reaching the curve maximum J_m is:

$$t_m = l^2 / (10.9D) \quad (4)$$

The flux in the maximum is:

$$J_m = 5.922 \Delta t D J_\infty / l^2 \quad (5)$$

Compared with the traditional versions of the permeability method, the pulsed version requires less time for the experiment and allows higher resolving power and dynamics [3].

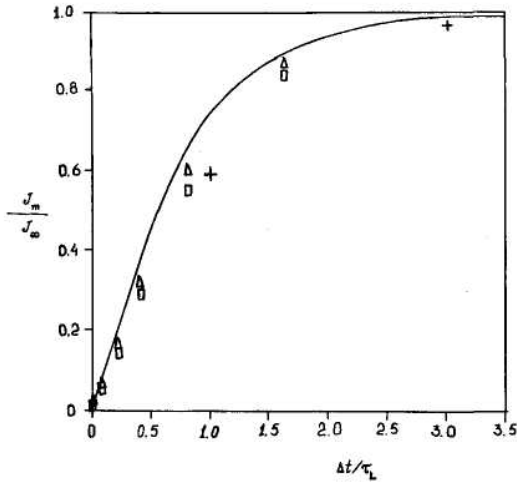


Fig. 1. Dependence of the exiting flux amplitude on time duration Δt of the square pulse of the gas concentration at the membrane inlet. (-) Theoretical curve; (\square) experimental data on CO_2 diffusion in PVTMS at carrier gas velocity $0.32 \text{ cm}^3/\text{sec}$; (Δ) experimental data on CO_2 diffusion in PVTMS at carrier gas velocity $1.61 \text{ cm}^3/\text{sec}$; (+) experimental data on He diffusion in PVTMS at carrier gas velocity $1.61 \text{ cm}^3/\text{sec}$.

Let us consider the passage of a square concentration pulse consisting of a binary gas mixture through the membrane. In this case the membrane acts as a chromatographic column. At the membrane outlet, separation of the mixture components takes place. Figure 2 shows, as an example, the results for two-component (A and B) gas mixture (50:50) concentration pulses of various time durations through the polymeric membrane. Let the permeability coefficients of gases A and B in the membrane be equal, $P_A = P_B$ (under steady-state conditions no separation of the mixture components occurs). Diffusion coefficients of these gases in the polymer are different: ($D_A = 10 D_B$) A is ten times more able to diffuse. Figure 2 shows that, at short times, component A is the main species present, at average times a mixture of components, and at long times, component B predominates. Figure 2 also shows that the peak resolution decreases with increasing pulse time duration. Thus the resolving power of the membrane cell can be controlled by selecting the pulse duration and adjusting the time intervals within which the choice of the output gas enriched with "fast" or "slow" gas mixture components is performed.

It is obvious that in the case of unsteady-state boundary conditions at the membrane inlet the classical selectivity coefficient is unacceptable.

For quantitative description of the membrane separation process under pulsed conditions, we introduce the term of differential unsteady-state selectivity coefficient:

$$\chi(t) = J_A(t) / J_B(t) = J_{A\infty} F_A / J_{B\infty} F_B = \chi_\infty K_x \quad (6)$$

$$F_i = f_i(u) - \alpha f_i(u - D\Delta t / l^2)$$

where $\chi_\infty = \sigma_A D_A / (\sigma_B D_B)$ is the steady-state selectivity coefficient, $K_x = F_A / F_B$ is the selectivity parameter, and $\chi(t) = K_x \chi_\infty$ is the differential unsteady-state selectivity coefficient.

It is clear that, at $\Delta t \rightarrow \infty$ and $t \rightarrow \infty$, $K_x \rightarrow 1$ and $\chi(t) = \chi_\infty$, i.e. at longer time durations of the concentration pulse at the inlet, the unsteady-state selectivity coefficient turns into the steady-state one. It is important to stress that χ_∞ is defined by the ratio of the permeability coefficients $P_A = \sigma_A D_A$ and $P_B = \sigma_B D_B$, while the K_x parameter is defined by the diffusion coefficients alone. Therefore, even when $P_A = P_B$, i.e. when the separation of gases is impossible under steady-state conditions, the separation of

the mixture (if $DA \neq DB$) proceeds quite efficiently under unsteady-state conditions.

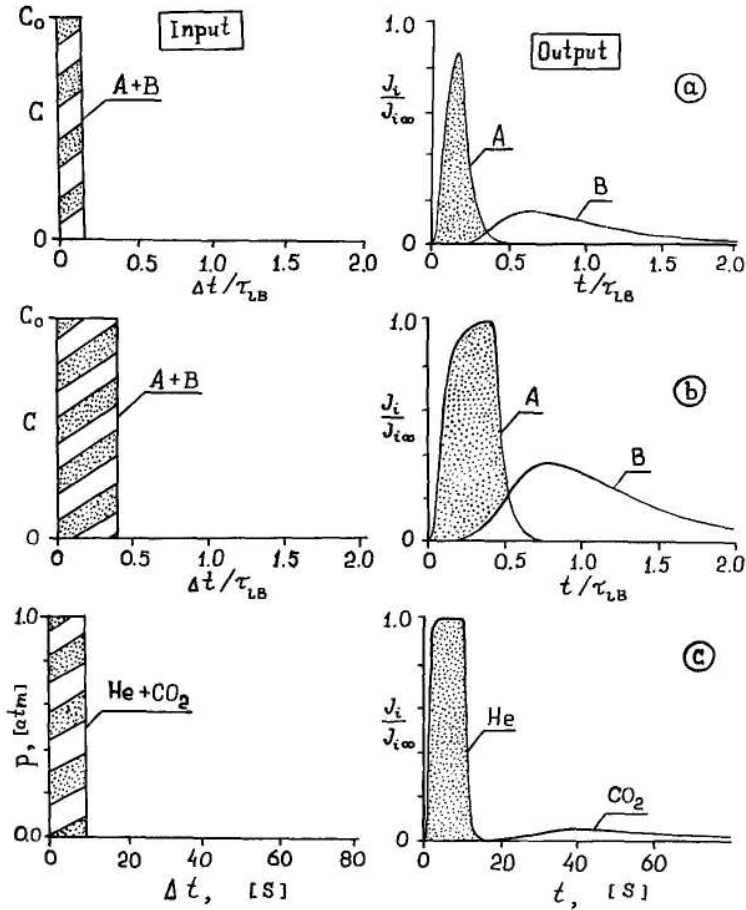


Fig. 2. Separation of two-component gas mixture under pulsed conditions, (a) Concentration pulse length $\Delta t = 0.15\tau_{LB}$; (b) concentration pulse length $\Delta t = 0.40\tau_{LB}$; (c) experimental data for He/CO₂ gas mixture diffusion.

Figure 3 shows the dependence of the selectivity parameter K_x on the pulse time duration and the time for selection of gases at the outlet from the membrane. A possibility of selectivity parameter inversion in the course of the experiment is obvious. It is seen that, at long time durations of the pulse and short measurement times, $K_x \gg 1$ (i.e. the outgoing flux is enriched with the "fast" component), while at short pulses and long diffusion times, $K_x \ll 1$ and the mixture is enriched in the component with the smaller diffusion coefficient.

Thus it follows that the pulsed version of the permeability method allows the separation of gas mixtures which fail to be separated under steady-state conditions, with the values of selectivity constants being very high.

Unfortunately, increasing selectivity leads to a decrease in membrane productivity. For this reason, in real conditions one should choose such magnitudes of pulse time duration and such times of component selection as would provide a compromise between productivity and selectivity [4].

We consider it reasonable to recommend the proposed method mostly for the application as separating membranes covering sensors, because increased selectivity results, rather than for industrial separation of gases. First of all, the membrane-sensor system requires very high selectivity factors, whereas a decrease in productivity is of less importance, since the sensor sensitivity is quite high.

Passage of concentration waves of gas mixtures

The method of concentration waves is based on study of the passage of harmonic oscillations of the penetrant concentration through the membrane. For example, if at the membrane inlet the gas concentration changes according to the sinusoidal law:

$$C = \frac{C_0}{2} [1 + \sin(\omega t)] \quad (7)$$

then at the membrane outlet the sinusoidal oscillation occurs at the same frequency, although with smaller amplitude and having suffered a phase shift (Fig. 4).

Under unsteady-state conditions, the flux changes at the membrane outlet according to the expression [5]:

$$J_t = \frac{DC_0S}{2l} \left\{ \sin(\omega t) + 2 \sum_{n=1}^{\infty} \frac{(-1)^n \left\{ \frac{n^2 \pi^2 D}{l^2} \left[\cos(\omega t) - \exp\left(\frac{n^2 \pi^2 Dt}{l^2}\right) \right] + \omega \sin(\omega t) \right\}}{\frac{n^2 \pi^2 D}{l^2} + \omega^2} \right\} \quad (8)$$

Periodic oscillations occur with respect to the level:

$$J_p = \frac{DC_0S}{2l} \left[1 + 2 \sum_{n=1}^{\infty} (-1)^n \exp\left(\frac{n^2 \pi^2 Dt}{l^2}\right) \right]$$

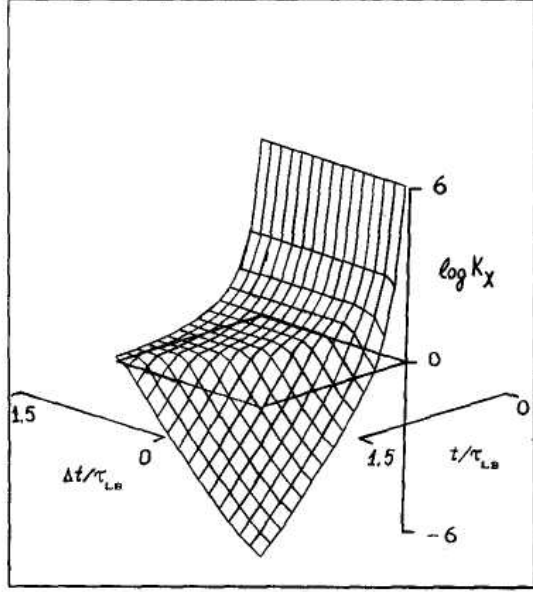


Fig. 3. Dependence of the selectivity parameter K_x on pulse duration Δt and measurement time t ($P_A=P_B$, $D_A = 10D_B$).

At long times, the steady-state condition is attained and is maintained with periodicity:

$$J_t = A \sin(\omega t + \phi) \quad (10)$$

where the amplitude A is given by:

$$A = \frac{(DC_0S/l)(l\sqrt{\omega/D})}{2[\sinh^2(l\sqrt{\omega/2D}) + \sin^2(l\sqrt{\omega/2D})]^{1/2}}$$

the phase shift ϕ is given by:

$$\phi = \arcsin \left[\frac{\cos(z)\sinh(z) - \sin(z)\cosh(z)}{\sqrt{2[\sinh^2(z) + \sin^2(z)]}} \right]$$

and $z = l\sqrt{\omega/2D}$

At high ω : $l\sqrt{\omega/2D} > \pi/2$ and $\phi \approx l\sqrt{\omega/2D} - \pi/4$, at low ω : $\phi = \omega l^2/(6D)$.

As compared with the classical version of the permeability method, the method of concentration waves exhibits additional degrees of freedom: the time of output towards the periodical steady-state condition, the equilibrium position, the oscillation amplitude and the phase shift [6, 7]. An additional degree of freedom results from the possibility of performing the experiment at various frequencies. Figure 5 exemplifies frequency characteristics (amplitude and phase) of the membrane at various values of the diffusion coefficient. It is seen that, with an increase of frequency, ω , the amplitude of the outgoing wave decreases (the lower the value of D , the faster the drop of the amplitude), while the phase shift passes through a minimum (with further increase of frequency, oscillation takes place). Thus, the membrane can be considered as a filter of low frequencies, and the greater the diffusion coefficient, the wider is the band of filtration.

The concentration waves diminish with an increase of frequency. However, the concentration waves exhibit all the properties of waves, in particular interference and diffraction. These effects are determined by the wavelength $\Lambda = 2\pi\sqrt{2D/\omega}$. The wavelength and, consequently, the conditions of diffraction can be changed by varying the oscillation frequency.

Now we consider the passage of the concentration wave through the membrane, where the wave consists of a mixture of two gases, A and B.

At the membrane inlet:

$$C_A = \frac{C_{A,0}}{2} [1 + \sin(\omega t)]; \quad C_B = \frac{C_{B,0}}{2} [1 + \sin(\omega t)] \quad (11)$$

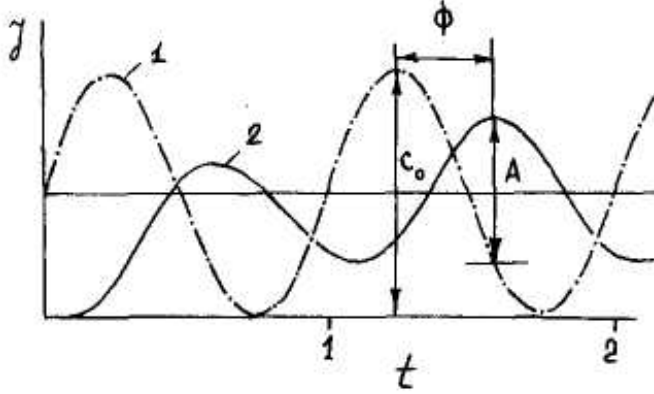


Fig. 4. Passage of the concentration wave through the membrane. (1) Change in gas concentration at the membrane inlet; (2) change in penetrant flux at the membrane outlet.

Then the flux at the membrane outlet is:

$$J_T = J_A + J_B \quad (12)$$

after the periodical steady-state condition is attained, and the oscillation amplitude is:

$$B_T = B_A \sin(\omega t + \phi_A) + B_B \sin(\omega t + \phi_B) = B_{AB} \sin(\omega t + \phi_{AB}) \quad (13)$$

where $B_{AB} = B_A^2 + B_B^2 + 2B_A B_B \cos(\phi_B - \phi_A)$

$$\phi_{AB} = \arctan\left(\frac{B_B \sin(\phi_B - \phi_A)}{B_A + B_B \cos(\phi_B - \phi_A)}\right)$$

where B_A , B_B and ϕ_A , ϕ_B are estimated by eqn. (10).

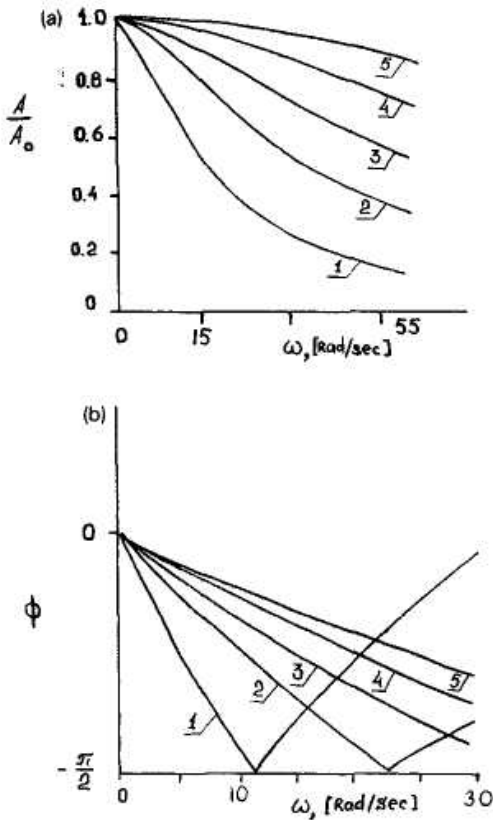


Fig. 5. Frequency characteristics of the membrane at various values of D/l^2 : (a) amplitude-frequency characteristics; (b) phase-frequency characteristics.

No.	1	2	3	4	5
D/l^2	1.26	2.51	3.98	6.31	10.0

Figure 6 illustrates the amplitude-frequency characteristic of the membrane for the mixture of gases A and B at various values of D_A/D_B (ratio of the mixture at the membrane inlet $A/B = 50:50$). Calculations were performed for $P_A = P_B$ (separation of the gases under steady-state conditions does not occur). It is seen that the oscillation amplitude of the gas mixture at the membrane outlet at decreasing wave frequency ($\omega \rightarrow 0$, $B_{AB}/B_A \rightarrow 2$) will be determined by both components of gas mixture. With the frequency ω increasing, the dependent $B_{AB}(\omega)/B_A$ passes through a minimum, and at $\omega \rightarrow \infty$, $B_{AB}/B_A \rightarrow 1$. The minimum point on the curve of the dependence of $B_{AB}(\omega)/B_A$ on ω is due to the fact that the phase shift between the output oscillations of components A

and B: $\Delta\phi = |\phi_A - \phi_B| \rightarrow \pi/2$, results in a decrease of the total value of the output oscillation amplitude.

At sufficiently high frequency ω , amplitude B_B for the component with the lower diffusion coefficient is small and the total amplitude of the output oscillations, B_T , is determined mainly by the amplitude for the mixture component with a higher diffusion coefficient.

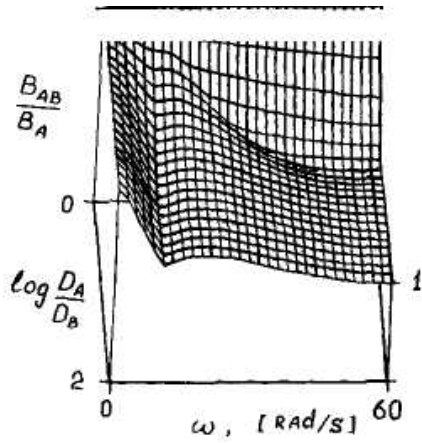


Fig. 6. Dependence of the normalized amplitude, B_{AB}/B_A , of the concentration wave which passed through the membrane at frequency ω , and the ratios of the diffusion coefficients of the gas mixture components D_A/D_B ($P_A=P_B$, and the gas mixture composition at the membrane inlets A:B = 50:50).

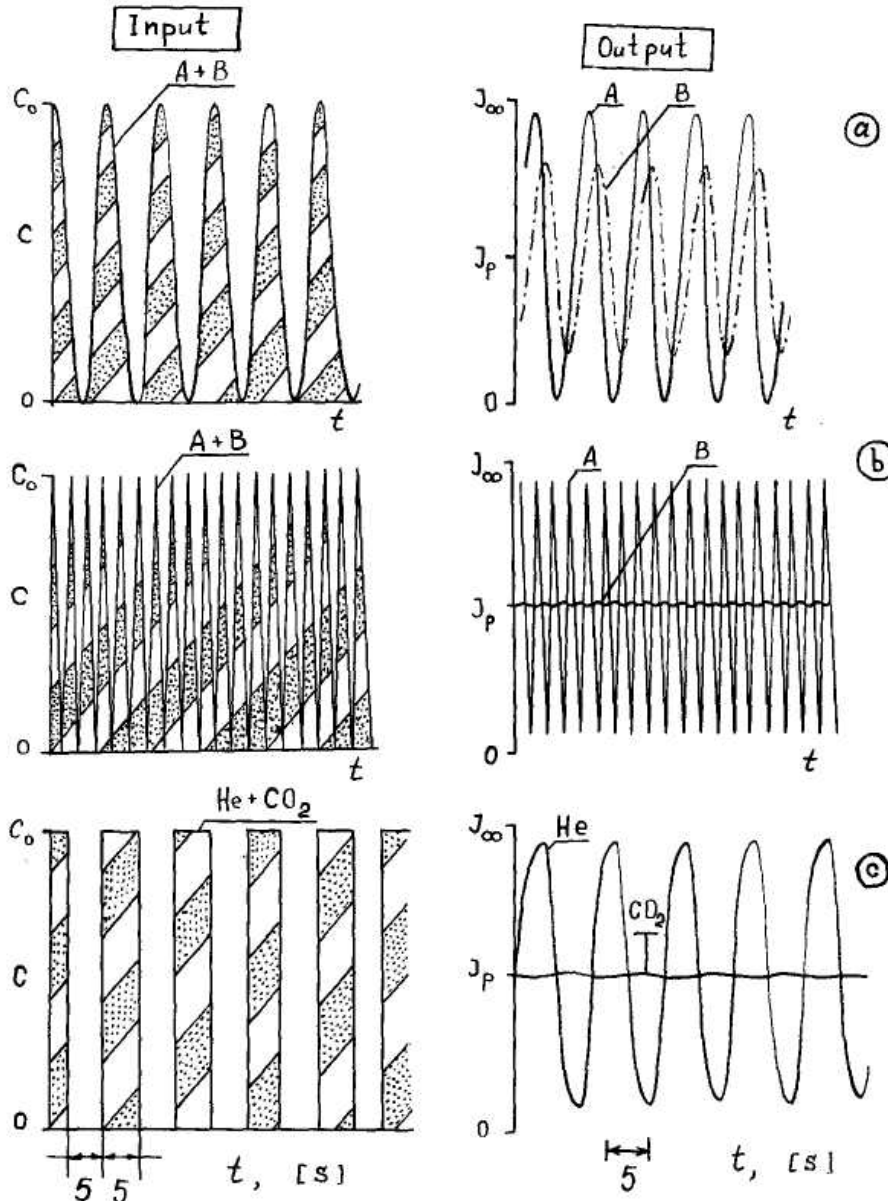
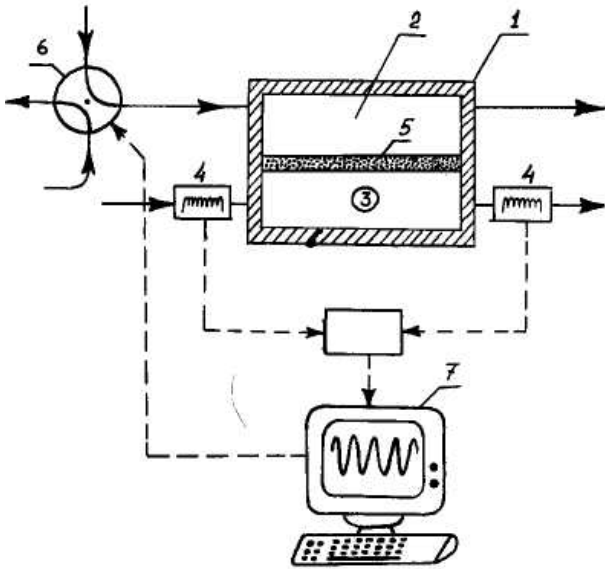


Fig. 7. Passage of the concentration wave of a mixture of two gases through the membrane at various frequencies: (a) oscillation frequency $\omega=5$ ($P_A=P_B, D_A=10 D_B$); (b) $\omega=60$ ($P_A=P_B, D_A=10 D_B$); (c) experimental data on the He/CO₂ mixture at oscillation frequency $\omega=0.628$ (rad/sec).

Figure 7 illustrates the dependences of the emergent flux at the membrane outlet of the gas mixture components for which the permeability coefficients in the membrane are equal and the diffusion coefficients differ by a factor of 10 ($D_A = 10D_B$). It is seen that, when the frequency increases from 5 to



60 rad/sec, the oscillation amplitude for the component with lower D drops abruptly, whereas for the component with a higher D the amplitude decreases negligibly.

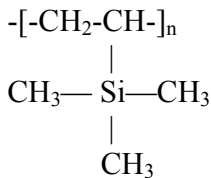
Fig. 8. Diagram of the experimental apparatus for separation of gas mixtures under unsteady-state conditions.

Thus, filtration of the output oscillations from the signal of the component of low D is attained by changing the frequency of the input oscillations of the concentration wave. The diagram of the apparatus used for the experiments is given in Fig. 8. The polymeric membrane (5) separates the diffusion cell (1) into two parts: the reservoir (2) and the collector (3). The carrier gas is supplied into the reservoir and the collector. At certain

intervals the carrier gas is replaced by the gas mixture according to a signal from the computer (7) turning the switched valve (6). The flux of the penetrant at the membrane outlet is detected by katharometer (4) and is stored in the computer memory. The diffusion cell is placed in an air thermostat with the temperature maintained within $\pm 1^\circ\text{C}$. The membrane surface area is 28.3 cm^2 . Both the reservoir and collector volume are equal to $\approx 0.5\text{ cm}^3$.

Results and discussion

Experimental verification of the proposed techniques was carried out with the use of polyvinyltrimethylsilane (PVTMS) film ($l=147\mu\text{m}$) as a membrane. The chemical structure of PVTMS is



The investigation was performed on a He/CO₂ gas mixture comprising 47% He and 53% CO₂. The main transport parameters of He and CO₂ in PVTMS are given in Table 1.

As may be seen from Table 1, the permeability coefficients of He and CO₂ are approximately equal, while the diffusion coefficients differ 74-fold.

Measurement technique

The katharometer exhibits a non-uniform sensitivity in detecting He and CO₂. For this reason, in our experiments we measured separately the output signal of He and the output signal of CO₂ under various boundary conditions at the membrane inlet. Helium was initially used as a carrier gas, and the CO₂ output signal was recorded after the He/CO₂ mixture passed through the membrane. The output signal of He was recorded after the substitution of the carrier gas for CO₂. The dependences of the flux velocity on time obtained in the experiment were normalized as to the penetrant flux under steady-state conditions:

$$J(t) = \frac{J_i(t)}{J_{i\infty}}$$

where $J_{\xi}(i)$ is the flux of the i -th component at the outlet from the membrane, and $J_{i\infty}$ is the steady-state

flux of the i -th component at the outlet of the membrane.

TABLE 1 Transport parameters of He and CO₂ in polyvinyltrimethylsilane

Gas	Permeability ^a	Diffusion coeff. ^b
He	$1.8 \cdot 10^{-8}$	$370 \cdot 10^{-7}$
CO ₂	$1.9 \cdot 10^{-8}$	$5.0 \cdot 10^{-7}$

^aP, cm³-cm/(cm²-sec cmHg). ^bD, cm²/sec.

Separation by the pulse method

Concentration pulses of penetrant (He/CO₂) with time duration $\Delta t = 5, 10, 15, 30, 60$ or 120 sec in the case of CO₂ and $\Delta t = 1, 3, 5$ or 10 sec in the case of He were applied at the inlet to the membrane cell. The velocity of the carrier gas in the collector and reservoir was equal to 0.32 cm³/sec. The dependence of the CO₂ output signal amplitude on the time duration of the pulse under these conditions is given in Fig. 1. It can be seen that the experimental data are located below the theoretical curve, apparently due to apparatus inertia (non-ideal gas flows in the collector and reservoir, e.g. deviations from plug flow) as well as to pulse dilution in passing over the membrane. It should be noted that the apparatus inertia distorts the kinetic curves of He much more than those of CO₂. With increasing velocity of the gas flux in the collector and the reservoir the sluggishness of the system decreases and the correlation between theory and experiment becomes better. With a further increase in velocity of the fluxes the detector sensitivity dropped abruptly. For this reason all the experiments were performed at a gas flux velocity of 1.61 cm³/sec.

The separating power of the PVTMS membrane when the He/CO₂ mixture concentration pulse is applied at the inlet is illustrated in Fig. 2 (c). One of the plots depicts the He and CO₂ outlet signals upon application of concentration pulses of 10 sec duration. As seen from the figure, the separation of the He/CO₂ mixture proceeds with sufficient efficiency.

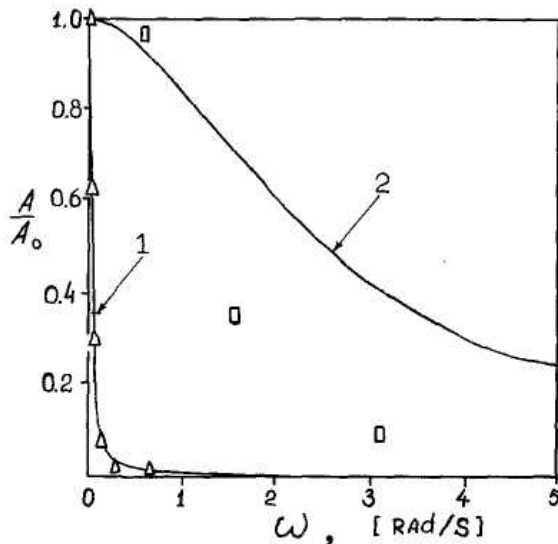


Fig. 9. Amplitude-frequency characteristics for the He/CO₂ mixture in the PVTMS membrane, (Δ) Experimental results with respect to diffusion of CO₂; (\square) experimental results with respect to diffusion of He; (1) theoretical amplitude-frequency characteristic for CO₂ in PVTMS; (2) theoretical amplitude-frequency characteristic for He in PVTMS.

Sinusoidal inlet boundary conditions

For technical reasons, the creation of concentration waves at the membrane inlet is difficult. Therefore, to investigate the amplitude-frequency characteristics of the He/CO₂ mixture in PVTMS, we employed as boundary conditions continuous concentration pulses (square wave oscillations) occurring at equal intervals. The flow velocities of the carrier gas and the penetrant were equal to 1.61 cm³/sec. As with the case of pulsed application of the penetrant concentration, the output signals of He and CO₂ were recorded separately. The frequencies ω (rad/sec) used in the experiments were equal to $0.026, 0.052, 0.105, 0.209$ and 0.628 for CO₂ and $0.628, 1.57$ and 3.14 for He.

The amplitude-frequency characteristics for He and CO₂ are given in Fig. 9. At a frequency above

≈ 0.77 rad/sec the oscillation amplitude $B_{\text{CO}_2} < 1\%$ of the maximum value, while the amplitude of the output oscillations of He, B_{He} is equal to $\approx 90\%$. Figure 7 illustrates the dependence of the input and output signals of the He/CO₂ gas mixture on time, with the frequency of the inlet oscillations ω being equal to 0.628 rad/sec. It is seen that under these conditions the detector records only the signal coming from He.

Conclusion

In the present work we have made an effort to consider some aspects of applying unsteady-state boundary conditions at the membrane inlet. The application of unsteady-state boundary conditions provides active control over the processes of gas transfer into the membrane. It has been shown that it also allows a considerable increase in the coefficient (by a factor of several orders) of separation of He/CO₂ gas mixtures in a non-selective polyvinyltrimethyl-silane membrane under unsteady-state boundary conditions.

The application of unsteady-state boundary conditions at the membrane outlet also offers prospects for membrane technology, since it allows a significant increase in the selectivity of the gas separation process with only a small decrease of its productivity.

The application of unsteady-state boundary conditions at the outlet of the membrane will be considered in future communications.

List of symbols

A	amplitude of oscillations for single gas
B_i	amplitude of oscillations for i -th component of gas mixture
B_T	total amplitude of oscillations
C_A, C_B	concentration of A and B gases at the inlet of the membrane
C_0	concentration of penetrant at the membrane inlet
D	diffusion coefficient
D_i	diffusion coefficient of i -th gas component
l	membrane thickness
J_A, J_B	transmembrane fluxes of components A and B
$J_{A\infty}, J_{B\infty}$	steady-state transmembrane fluxes of components A and B
J_m	maximum penetrant flux
J_∞	steady-state diffusion flux
K_x	selectivity parameter
p	partial pressure
P_i	permeability coefficient of i -th gas component
Δt	impulse duration
t	time
S	membrane area
σ	solubility coefficient
σ_i	solubility of i -th gas component
ϕ	phase shift
ω	frequency of oscillation concentration at the membrane input
χ_∞	steady-state selectivity coefficient
$\chi(t)$	differential unsteady-state selectivity coefficient
τ_L	time-lag
τ_{LB}	time-lag for diffusion of B component of gas mixture

References

- 1 G. Palmai and K. Olah, New differential permeation rate method for determination of membrane transport parameters of gases, J. Membrane Sci., 21 (1984) 161.
- 2 IN. Beckman, I.P. Romanovski and V. Balek, Diffusion methods in the defectoscopic study of

- selective membranes, in: B. Sedlazeck and J. Konovec (Eds.), *Synthetic Polymeric Membranes*, Walter de Gruyter, Berlin, 1987, p. 355.
- 3 I.N. Beckman and V. Balek, Diagnostics of gas separated membranes using inert gas probe methods, 1987 International Congress on Membrane and Membrane Process, Tokyo, Japan, June 8-12, 1987, p. 524.
 - 4 A.B. Shelekhin, I.N. Beckman and V.V. Teplyakov, Separation of gas mixtures under unsteady-state conditions, in: *Preprints, International Symposium on Membranes for Gas and Vapour Separation*, Suzdal, U.S.S.R., 1989, p. 61.
 - 5 I.N. Beckman, I.E. Gabis, T.N. Kompaneets, A.A. Kurdyumov and V.I. Lyasnikov, Investigation of hydrogen permeability in the technology for the production of electronics, in: *Reviews on Electronics, Ser.: Technology, Production, Management and Equipment*, Elektronika, Moscow, 1985, No. 1, p. 66.
 - 6 I.N. Beckman, The mass-transfer control in membranes, in: *Preprints, International Symposium on Membranes for Gas and Vapour Separation*, Suzdal, U.S.S.R., 1989, p. 24.
 - 7 R. Paterson and P. Doran, A. new method for determining membrane diffusion coefficients from their response to regular forced concentration waves, *J. Membrane Sci.*, 27 (1986) 105.